

Structural-thermal FE simulation of vibration and heat generation of cracked steel plates due to ultrasound excitation used for vibrothermography

by R. Plum* and T. Ummenhofer*

*Karlsruhe Institute of Technology, Versuchsanstalt fuer Stahl, Holz und Steine, Otto-Ammann-Platz 1, 76128 Karlsruhe, Germany, robin.plum@kit.edu, thomas.ummenhofer@kit.edu

Abstract

A major drawback of ultrasound excited thermography applied to metal components manifests in the pronounced frequency dependence of crack detectability. In order to investigate the crack face interaction by which it is constituted whether a certain crack can be detected or not structural-thermal Finite Element simulations of a massive steel plate are conducted using ANSYS/LS-DYNA considering the physical roughness of the crack faces. The achieved numerical results are in a good agreement with experimental data of a performed ultrasonic sweep thermography (UST).

1. Ultrasound excited thermography

Ultrasound excited thermography or vibrothermography is known to be a fast non-destructive testing method which has been successfully applied to components made of FRPs, metals and many other engineering materials in order to detect cracks, delaminations or other types of internal flaws [1, 2]. Focusing on metals, ultrasound excited thermography testing has already been used for industrial routine testing of repetition parts although the mechanisms of heat generation at crack locations are not identified exactly. Vibrothermography has been applied in the way of a mobile testing system as well. A 3.2 m long hot-rolled girder IPE 500 showed its cracks even if the excitation is applied in a distance of 2.5 m. However, the investigation of heavy steel members used in constructional steelwork like plates and girders revealed that the location of excitation and the coupling method influences the thermographic detectability of through-thickness cracks [3]. Generally the amount of heat generation at the cracks is strongly dependent on the ultrasonic frequency as several researchers found out in the past [3, 4]. These effects lead to an uncertainty in the mobile use of vibrothermography concerning reproducibility and reliability. One of the main purposes of future investigations in this field is the detailed understanding of the crack face displacements and interaction which depend on the global vibration behaviour of the stimulated component.

2. Experimental investigations

2.1. Specimen

Since a reference measurement is required for comparison with the numerical simulation a steel plate of (European) grade S355J2+N with dimensions as shown in figure 1 was subjected to fatigue loading using a resonant testing machine. The desired depth of the through-thickness crack starting from the notch bottom was set to be 24 mm. Excessive crack propagation was prevented by controlling attached crack detection wires which trigger the machine to stop in case of rupture. The specimen was cyclically loaded with a maximum load of 120 kN at a stress ratio $R = 0.1$ to avoid buckling of the plate. Macroscopic crack propagation started at 405000 load cycles and the final crack depth was reached after additional 21000 cycles have been accumulated.

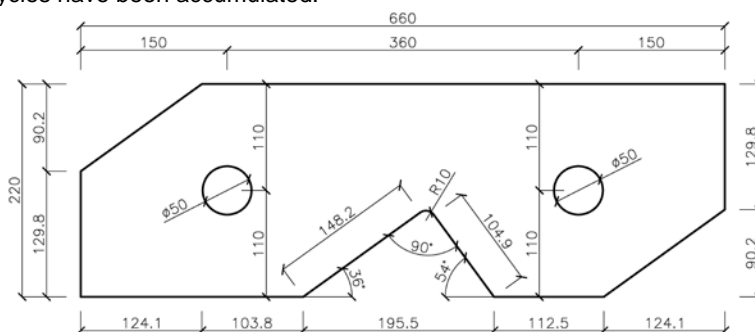


Fig. 1. Dimensions of the steel plate in mm; Thickness $t = 10$ mm

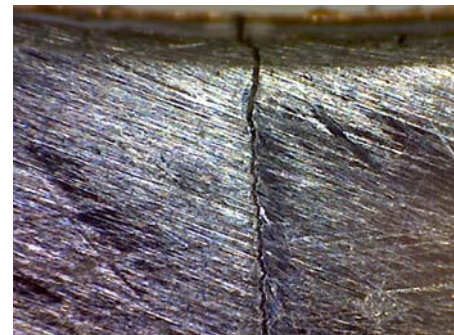


Fig. 2. Microscopic image of the cracked notch

The maximum crack opening at the notch bottom was found to be approximately 25 μm and 13 μm at the half crack depth. Hence, a linearly increasing crack opening can be assumed for modeling the crack. The best available set of relevant material parameters is given in table 1 and is taken from Wichers who worked with the same steel grade [5]. The parameters are used for FE modeling of the specimen described in section 3.

Table 1. Material parameters for carbon steel S355J2+N at 20 °C according to [5]

E [MPa]	ν []	ρ [kg/m ³]	C [J/(kg K)]	k [W/(m ² K)]
≈ 210000	0.277	7837	461	40.4

2.2. Thermographic crack detection

Exciting the plate by means of a BRANSON 2000b ultrasonic plastic welding system results in a strong and localized thermal response of the crack faces. It is shown in [3] and [4] that for metallic components a strong dependence on the ultrasonic frequency is to be expected. A 50 s ultrasonic sweep thermography in the range from 19 to 23 kHz was performed and revealed that intense crack heating occurs at several delimited frequencies only. Figure 3 illustrates the local heating where the crack path is approximately given by the straight line A – B. Subfigures (a) and (b) show the maximum temperature and the maximum temperature difference reached, respectively. As proposed in [4] the visibility of defects can be improved by mapping the maximum values of the first temporal or frequency derivative of each pixel signal obtained during the frequency sweep (figure 3 (c)). This method turns the imaging to be strongly defect-selective if sound parts of the specimen and the background do not increase in temperature. Alternatively figure 3 (d) shows the integral values of the temperature difference of each pixel signal which clearly identifies the location of maximum heat generation. Figures 4 and 5 illustrate the history of the maximum temperature difference achieved globally and along the line A – B, respectively.

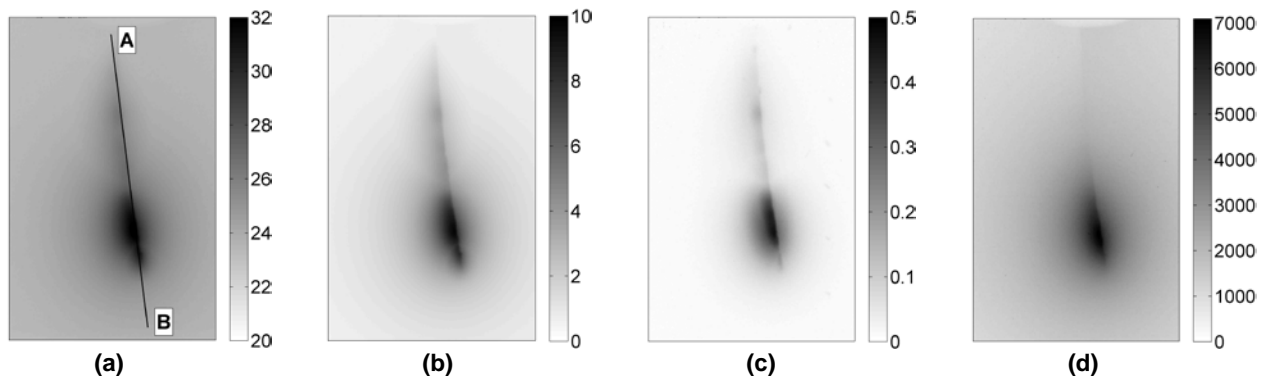


Fig. 3. Thermographic crack detection: (a) Max. temperature [°C]; (b) Max. temperature difference [K]; (c) Max. value of 1st derivative with respect to frequency [K/Hz]; (d) Integral value of temperature differences [K Hz]

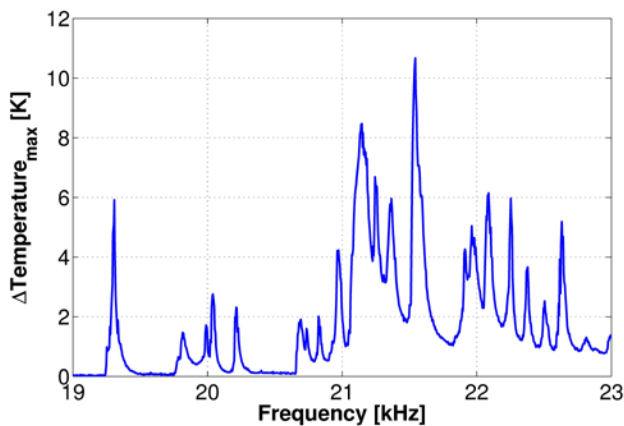


Fig. 4. History of the max. temperature difference

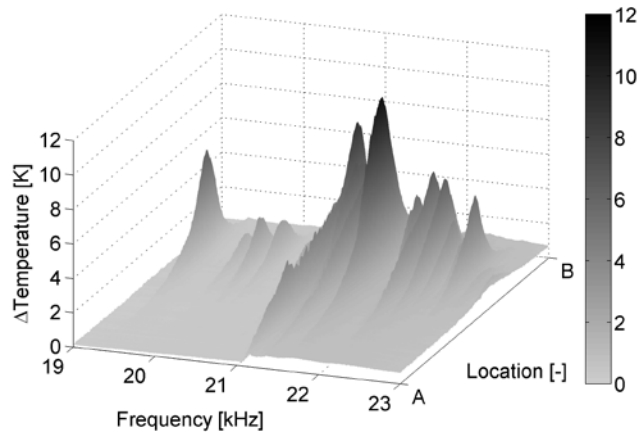


Fig. 5. Max. temperature difference along A - B

3. Numerical Simulation

3.1. Simulation approach

The high frequency mechanical excitation of the steel plate, its transient oscillation and the local heating at the crack region is simulated by a three step approach using ANSYS/LS-DYNA 12.0. The software allows decoupling of the mechanical and the thermal problem and the use of explicit time integration. Three distinct finite element models are built:

- Global mechanical model of the cracked plate with rather coarse mesh of the crack region (figures 8, 10)
- Partial mechanical model of the crack region with fine mesh of the crack faces (figures 11, 14) where the node numbers of the outer regions correspond to the node numbers of the global model
- Partial thermal model of the crack region having exactly the same mesh and node numbers as the partial mechanical model

At first the purely mechanical part of the experiment is simulated. The coupled system of ultrasonic transducer and steel plate needs several vibrations periods to turn from a transient to a steady state oscillation. The simulation time step size dt is chosen to be $T/20$ with T being the cycle period. A Complete simulation of a 0.1 s excitation would require 40000 time steps to be calculated. Since the computational cost is high using a detailed three dimensional model of the cracked plate a different approach is pursued. It is assumed that the plate reaches a steady state after 100 sinusoidal excitation periods. Hence, the first 100 periods are simulated using the complete mechanical model (figure 8) without saving any results. Continuing the explicit FE simulation the nodal displacements for five additional periods are stored.

Next, the partial mechanical model with finer mesh of the crack region is run for five periods. The nodal displacements obtained from the explicit model are transferred to the outer region of the partial model and directly used as boundary conditions. This way the partial model is forced to move like the global model. The reactions of the inner region of the model which contains the crack faces and the crack tip can arise freely in the transient analysis. The crack faces are equipped with surface-to-surface contact and target elements, respectively. ANSYS directly outputs the friction stress τ and accumulated sliding distance s for each contact element based on a COULOMB friction law. These outputs are systematically stored and used for calculation of the resulting heat flux H on the contacting crack faces due to dry friction on a per-element basis. The surface element heat load H is given for every time step i as:

$$H_i = \frac{\tau_i}{2} \cdot \frac{|s_{i-1} - s_i|}{dt} \quad (1)$$

A division by two takes into account that the generated heat spreads out in two opposing crack faces. Since the partial model is subjected to inertia forces as well only the last three of the five simulated periods are monitored. With the assumption of a steady state oscillation the friction heat load history H_i can be averaged over time.

As a last step the calculated heat loads are transferred to the thermal model which has the same node and element numbering as the structural model. Again, a transient calculation performed with a free choice of the time stepping and the final simulation is done resulting in the spatially resolved heat diffusion. The thermal calculation method was verified by a simple model of two blocks sinusoidally sliding on each other. Figures 6 and 7 show the heatflux and the increase in temperature at one point comparing a thermo-structural model using ANSYS coupled elements, a set of decoupled models and the decoupled models using averaged heat loads.

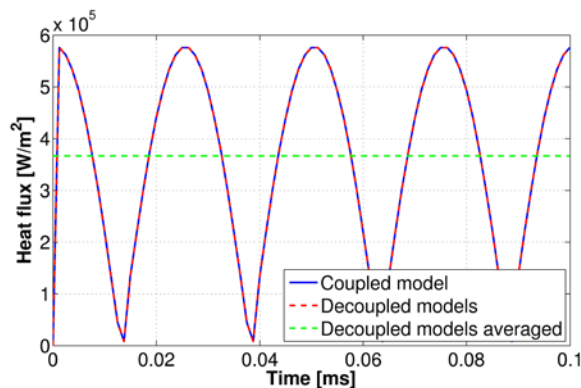


Fig. 6. Evolution of the heat flux at one point

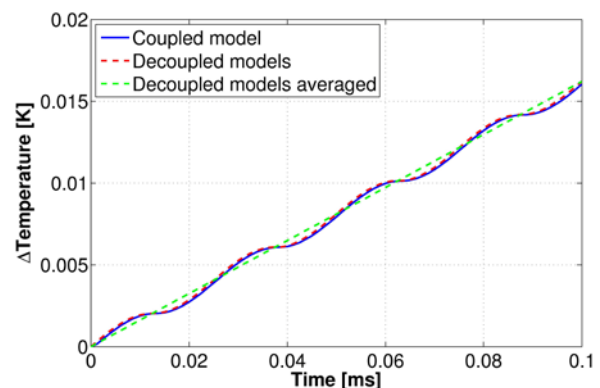


Fig. 7. Temperature increase at one point

3.2. Finite Element modeling

Ultrasonic transducer and steel plate are forming a rather complex oscillating system. The converter with its piezo element stack inside is not modeled within this work. From the authors' point of view it is very expensive to realistically simulate the complex vibrational characteristics of an ultrasonic transducer. However, Han et al. presented some FE models including a simplified transducer [6]. Several other simulation attempts showed promising results as well [7, 8]. As a first approach the cracked steel plate is three-dimensionally modeled using ANSYS/LS-DYNA explicit dynamic elements SOLID164 (8-node brick solid) and COMBI165 (2-node spring-damper). Since within an explicit simulation the smallest element size is critical for the internal time stepping and the complete structural model should only be able to reproduce the global dynamics of the plate the element size is chosen to be moderate as depicted in figure 8. Along the plate thickness four divisions are used (compare figure 14). It has been found that the element size is suitable for simulating vibrational modes at the 20 kHz regime as figure 9 shows a smooth bending shape. Here, the crack region is not refined and the through-thickness crack is realized as a simple cut with length of 24 mm. When using the LS-DYNA solver the definition of the crack face contacts does not require contact and target elements as it is known from an implicit FE analysis.

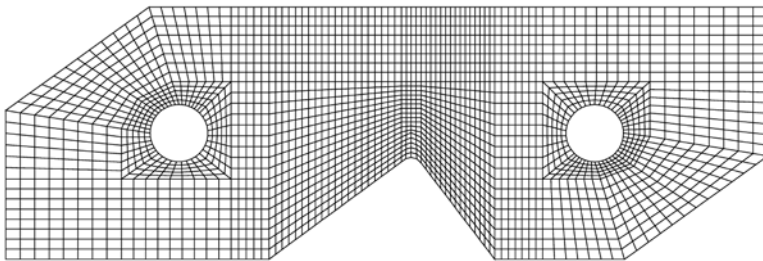


Fig. 8. Global FE model of the steel plate

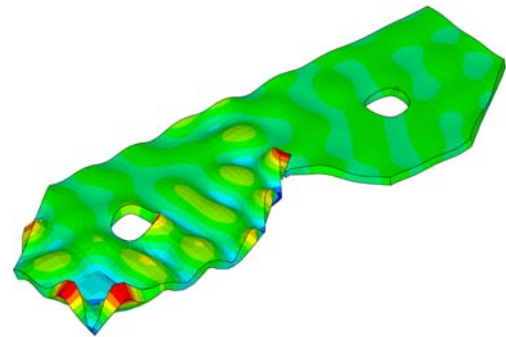


Fig. 9. Out-of-plane displacement (1000x)

The partial structural and thermal implicit models are based on the explicit model shown above. The fundamental distinction can only be found in the discretization of the crack region. In order to resolve the crack face interaction properly this region is strongly refined. Since we do not take plasticity into account at this time the crack front is modeled by dragged singular elements which are arranged fan-like around the crack tip and allow for calculation of the stress intensity factors. However, the SIF calculation under static loading is not relevant in this context. In order to transfer nodal displacements from the global model to the partial structural model a certain region of both models has to match each other's node locations and numbers. The figures 10 and 11 show the notch region of the global model and the partial model identifying their different inner crack regions (bright elements).

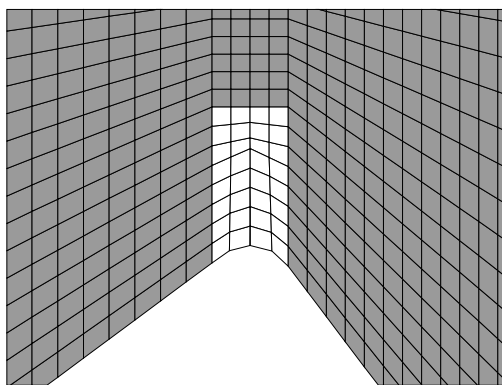


Fig. 10. Notch region of the global FE model

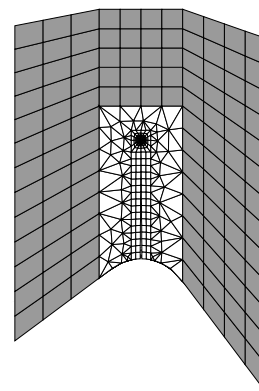


Fig. 11. Partial FE model

Both structural models are highly parameterized allowing to adjust the crack orientation, its position offset from the notch bottom and of course the crack opening at the beginning and at 90 % of the crack depth. The crack line is assumed to be straight although experiments revealed that they are often kinking to some extent. Additionally a "physical" roughness of the crack faces is implemented by randomly moving the nodes of both faces in space orthogonally to their planes. This is not a standard routine and care has to be taken since existing elements are deliberately distorted which might result in poor

element performance. However, node locations can be altered to some fraction of the element edge length without encountering any problems. Thompson proposed four different methods of generating rough surfaces in ANSYS and analyzed the contact behavior when pressed against a perfectly flat and rigid surface [9]. Figures 12 and 13 depict two of the methods which have been considered for implementation. Both surfaces on the top of the blocks are generated by the same pattern of asperities. The block on the left hand side was built from the bottom up with free tetrahedral meshing afterwards, the one on the right hand side is constructed top down using a simple block volume, mapped brick meshing and subsequent node modification.

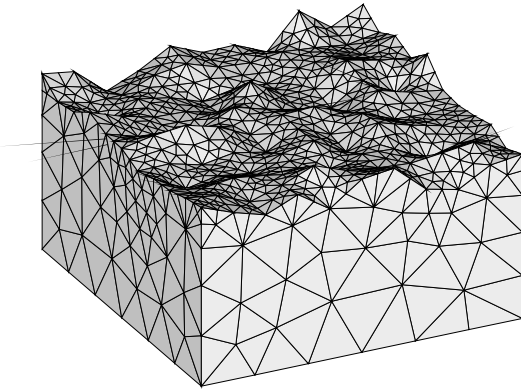


Fig. 12. Rough surface using bottom up modeling

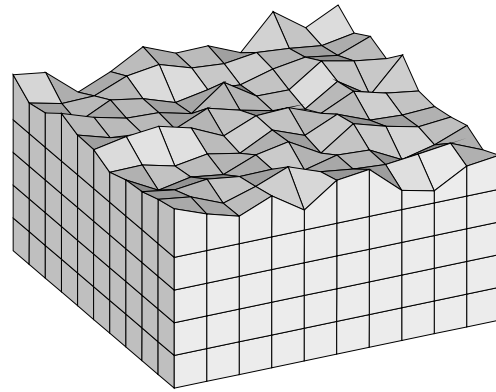


Fig. 13. Rough surface using top down modeling

The second version was used within the models because the structural error in case of contact is almost as low as in the other version and because bottom up modeling is rather expensive when all other volumetric components are generated by geometric primitives using the top down modeling approach which is the most common. Moreover the number of contact elements is much less which reduces the computation time. Figure 14 illustrates the detailed crack modeling for the implicit models. Note that the maximum asperity height as well as the crack opening are exaggerated for better visibility. Figure 15 shows a typical random distribution of asperities generated by ANSYS using a GAUSSian distribution with a standard deviation of 0.33. Approaching the crack front the asperities are omitted in order to comply with the straight front and to prevent distortion of the singular crack tip elements. The asperity map can be freely scaled in magnitude to simulate different surface roughnesses.

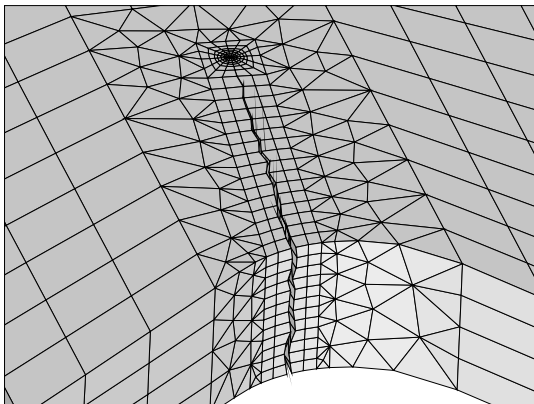


Fig. 14. Partial model with rough crack faces

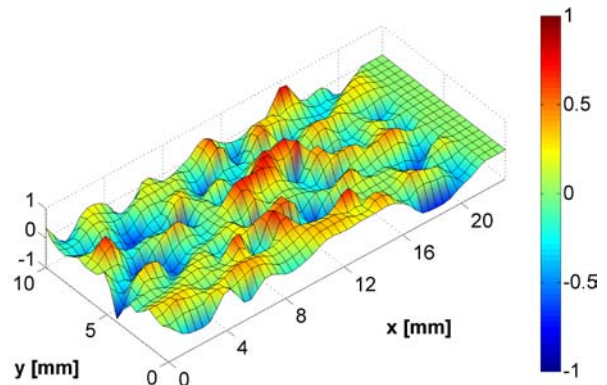


Fig. 15. Unscaled random distribution of asperities

For building the structural implicit model ANSYS elements SOLID185 (8-node brick solid), SOLID186 (20-node brick solid), SOLID192 (10-node tetrahedral solid), CONTA173/174 (4/8-node surface-to-surface contact) and TARGE170 (target segment) are used.

The thermal model fully corresponds to the partial structural model. Only the element types have been switched from structural to thermal. ANSYS elements SOLID70 (8-node brick solid), SOLID90 (20-node brick solid), CONTA173/174 (4/8-node surface-to-surface contact) and TARGE170 (target element) are used. The heat fluxes which are calculated for each contact element are automatically applied to both of the crack faces so that a symmetrical heat dissipation is achieved.

3.3. Loading and boundary conditions

As a first approach the mechanical loading of the steel plate is simulated by simply moving surface nodes within a circular area (the contacting surface of the transducer tip) sinusoidally in the out-of-plane direction. The excitation is simulated in a distance of 70 mm from the lower left corner of the plate shown in figure 1. A displacement amplitude of 15 μm is chosen. The plate is vertically supported and clamped by several pieces of very soft foam. The Young's modulus E of this foam was estimated to be 5 MPa which is an average value for polystyrene. In the explicit FE model spring-damper elements (COMBI165) with a length of 10 mm are attached at the corresponding positions. The spring stiffness k_s is evaluated from the dimensions of the foam blocks which have a thickness t of about 10 mm and a section area A of 15 x 15 mm. Structural damping of the supports is not considered yet.

$$k_s = \frac{E \cdot A}{t} \quad (2)$$

Gravity is not included in the simulation because the effects on the stress and displacement fields are considered to be negligible. Thermal energy losses due to convection and radiation are not taken into account because they do not affect the temperature distribution of the steel plate significantly. The heat flux density due to convection and radiation is estimated:

$$\dot{q}_{tot} = \dot{q}_c + \dot{q}_r = \alpha_c \cdot (T - T_{air}) + \varepsilon \cdot \sigma \cdot (T^4 - T_{env}^4) \quad (3)$$

where α_c is the unknown convective heat transfer coefficient, ε is the surface emissivity and σ being the STEFAN-BOLTZMANN constant. For an order of magnitude estimation of α_c the air temperature T_{air} and the temperature of the environment T_{env} is assumed to be 290 K whereas the steel plate temperature T is assumed to be 300 K. α_c can be determined indirectly by means of the definition of the dimensionless NUSSELT number Nu and the formula by CHURCHILL and CHU for estimation of Nu in case of a vertical wall or plate [10]:

$$Nu = \alpha_c \cdot \frac{L_0}{\lambda_{air}} \quad (4)$$

$$Nu_m = \left(0.825 + \frac{0.387 \cdot Ra^{1/6}}{\left[1 + \left(\frac{0.492}{Pr} \right)^{9/16} \right]^{8/27}} \right)^2 \quad (5)$$

L_0 is a reference length which is set to 50 mm. RAYLEIGH number Ra , PRANDTL number Pr and the coefficient of thermal conductivity of air λ_{air} can be looked up in textbooks e.g. [11] or can be calculated. In summary α_c was estimated to be 5.1 W/(m²K). A transient thermal simulation of a crack with uniformly distributed heat flux applied to the crack faces including convection and radiation resulted in a temperature decrease of about 10 mK compared to a simulation run without energy losses. The applied heat loading was adjusted before to make sure that a temperature increase of about 10 K is reached on the model surface. Hence, the effects of convection and radiation are ignored for the batched simulation runs described in the next section.

3.4. Batched simulation passes

A complete simulation pass consisting of (i) the global dynamic simulation, (ii) the refined structural analysis and (iii) the thermal simulation is only valid for one set of input parameters like excitation amplitude, ultrasonic frequency, crack opening and asperity distribution etc. As a first parameter study the frequency is varied from 19 to 23 kHz corresponding to the performed ultrasonic sweep thermography of the plate described in section 2. The frequency step size is 20 Hz and the thermal model is run up to 1 s simulation time with the averaged heat fluxes applied. Static and dynamic friction coefficients are set to 0.3, the maximum asperity height is chosen to be 50 μm and the maximum crack opening is 25 μm as mentioned in section 2. Running the 200 sets of simulations in a batch mode takes about 24 hours on a standard dual core PC. Most of the computation time is required for solving the partial implicit structural model. Results are presented in section 4.

4. Numerical results

For each time step of the implicit structural and thermal simulation various results are saved for further analysis. At first the temperature increase is compared to the conducted experiment. The ultrasonic sweep described in section 2 was done by raising the frequency in steps of 10 Hz. Theoretically each frequency level was held for 0.125 s whereas a short time is required for the ultrasound system to tune in the frequency set-point and for the vibrating system to reach a steady state. Thus, the simulated temperature distribution at 0.1 s which corresponds best is processed. Figure 16 depicts the maximum temperature differences obtained along the crack line on the model surface. A direct comparison with figure 4 reveals that the strong frequency dependence of the crack heating is matched very well. Furthermore the location of heat generation is in accordance with the experimental findings. Figure 17 shows the temperature distribution along the crack line after 0.1 s simulation time over frequency.

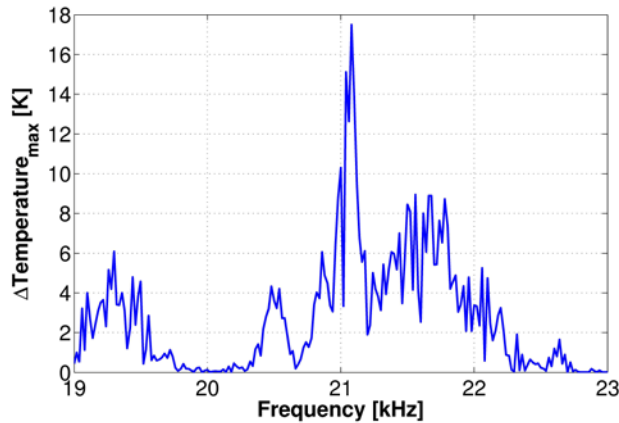


Fig. 16. Max. temperature difference [kHz] along crack line

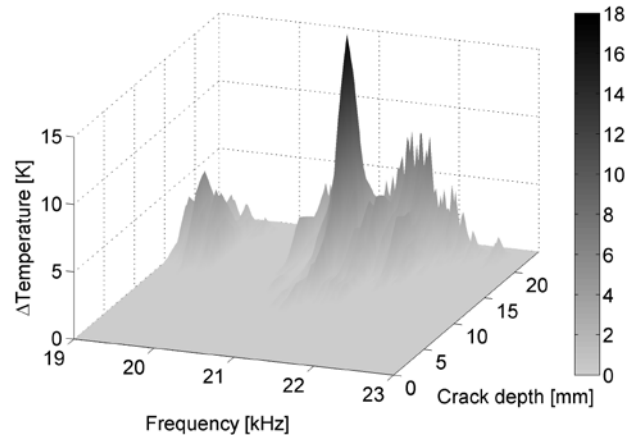


Fig. 17. Temperature difference along crack line

Exemplarily the crack face loading is presented for a frequency of 21.08 kHz in figure 18. The parameters are based on the contact elements used for the implicit structural simulation run regarding only the last periods which also allow for averaging the heat flux values. Since all crack face parameters are determined on a per-element basis and saved together with each element centroid the values are interpolated on a uniform grid for demonstration purposes. The subfigures map the maximum values of the heat flux, the contact pressure, the velocity and the friction stress. As the models do not include plasticity yet the stresses might exceed the yield limit of 360 MPa. This is the case for the contact pressure very close to the crack front (lower right corner). Velocity values are only defined (and greater than zero) in case of a sliding contact. The mappings in figure 18 reveal that only a few contact locations exist and that most of the crack face area is rather inactive referring to friction heat generation.

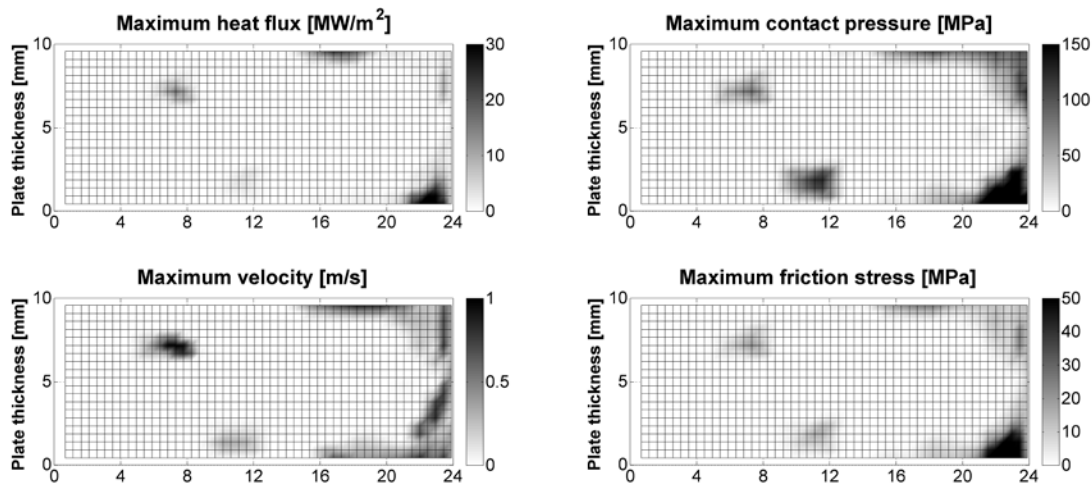


Fig. 18. Distribution of various parameters at the crack faces at $f = 21.08$ kHz

5. Summary and Conclusion

A finite element modeling scheme using ANSYS/LS-DYNA is proposed to completely simulate the ultrasound excited thermography applied to a massive steel plate. With the assumption that an oscillatory steady state is reached the highly dynamic excitation and vibration of the plate, the contact problem at the crack faces as well as the localized heat generation are approached. Concerning the thermal response of the crack region the numerical results are in a good agreement with experimentally achieved data from ultrasonic sweep thermography tests. As a main improvement the modeling of physical roughness at the crack faces is introduced. Randomly distributed asperities are implemented in the FE model resulting in spatially limited sliding contacts which lead to a realistic non-uniformly distributed friction heating. Furthermore the pronounced frequency dependence of the crack detectability manifests in the simulations. Comparing the numerical and experimental results it can be stated that the heat generation is slightly overestimated by the presented FE models. It has to be taken into account that the experimental sweep is done in a continuous fashion and the subsequent simulation runs are independent of each other. In practice frequencies are quickly swept and a previously hold frequency that leads to intense heat generation results in a heat diffusion that is superimposed on the heat generation at the next frequency set-point. However, it can be concluded that detailed Finite Element simulations might be able to predict the detection probability of a certain crack-like flaw within a metal component in the future. Furthermore the simulation can contribute to the assessment of detection limits, restrictions and vibrational conditions which have to be met in order to successfully detect cracks in metal structures using ultrasound excited thermography.

6. Outlook

This work will be continued since several effects have not been considered yet. The following tasks will be worked on in the future to provide more realistic modeling of ultrasound excited thermography testing:

- Comparison and adjustment of the plate displacements by means of scanning 3D laservibrometry
- Frequency analysis of the experimental and numerical crack face displacement components
- Implementation of RAYLEIGH damping in the explicit FE model
- Implementation of a more sophisticated friction law
- Implementation of cyclic plasticity
- Adjustment of the dynamic and thermal response of the model by means of synchronous laser vibrometry and IR thermography
- Switching to force control of the excitation and considering non constant excitation loading at varying frequencies

Acknowledgement

The authors gratefully acknowledge the financial support of this project by the German Research Foundation (DFG).

REFERENCES

- [1] Dillenz A., Busse G. and Wu D., "Ultrasound lock-in thermography: feasibilities and limitations", Diagnostic Imaging Technologies and Industrial Applications, Proceedings of SPIE, vol. 3827, p. 10-15, 1999.
- [2] Rantala J., Wu D., Salerno A. and Busse G., "Lock-in thermography with mechanical loss angle heating at ultrasonic frequencies", QIRT 96, Stuttgart, Germany, Proceedings, p. 389-393, 1996.
- [3] Plum R. and Ummenhofer T., "Ultrasound excited thermography of thick-walled steel load bearing members", QIRT Journal, vol. 6, no. 1, p. 79-100, 2009.
- [4] Gleiter A., Spiessberger C. and Busse G., "Improved ultrasound activated thermography using frequency analysis", QIRT Journal, vol. 4, no. 2, p. 155-164, 2007.
- [5] Wichers M., "Schweißen unter einachsiger, zyklischer Beanspruchung, Experimentelle und numerische Untersuchungen", Dissertation, University of Braunschweig, Germany, 2006.
- [6] Han X., Favro L.D. and Thomas R.L., "Finite-element modeling of acoustic chaos to sonic infrared imaging", Journal of applied physics, vol. 9, no. 1, 014907, 2005.
- [7] Mian A., Newaz G., Han X., Mahmood T. and Saha C., "Response of sub-surface fatigue damage under sonic load – a computational study", Composites Science and Technology, vol. 64, no. 9, p. 1115-1122, 2004.
- [8] Mabrouki F., Thomas M., Genest A., and Fahr A., "Frictional heating model for efficient use of vibrothermography", NDT&E International, vol. 42, no. 5, p. 345-352, 2009.
- [9] Thompson, M.K., "Methods for the generation of rough surfaces in ANSYS", Proceedings of the 2006 International ANSYS Users Conference & Exhibition, Pittsburgh, 2006
- [10] Baehr, H.D. and Stephan K., "Wärme- und Stoffübertragung", 5th edition, Springer, Berlin, Germany, 2006.